Journal of Physics: Conference Series

PAPER • **OPEN ACCESS**

Concentrated Solar Power (CSP) for Sustainable Architecture to Supply Domestic Hot Water and Heating Loads of Buildings

To cite this article: Hamidreza Zarrinkafsh *et al* 2021 *J. Phys.: Conf. Ser.* **2042** 012110

Concentrated Solar Power (CSP) for Sustainable Architecture to Supply Domestic Hot Water and Heating Loads of Buildings

Hamidreza Zarrinkafsh[1], Nasim Eslamirad[2], Francesco De Luca[3]
[1]School of Architecture, University of Tehran, Tehran, Iran
[2]Department Smart City Center of Excellence (Finest Twins), Tallinn University of Technology, Estonia
[3]Tallinn University of Technology, Estonia

zarinkafsh@ut.ac.ir

Abstract. Parabolic Trough Concentrators (PTC) are the most common solar concentrators. However, the high cost of production, operation, sun- tracking system, and the environmental sensitivity made them unprofitable for urban contexts. Lenses are more efficient and effective, but the complexity of manufacturing made them less used in sustainable architecture. This research proposes a liquid lens to be integrated into buildings' envelope and compared with a PTC based on the energy production and reduced CO_2 emissions over a year. The output energy, temperature, and efficiency of concentrator are obtained by the physics of light equations, and Ray-tracing software simulation. The results show that water lenses are at least 6% more efficient, their output temperature is higher, their underneath greenhouse effect made them less sensitive to the environment, and are still productive in high latitudes where PTCs are not operative. The paper presents the full result of the research that was registered as a patent.

1. Introduction

Integrating solar energy conversion equipment in an urban built environment has many challenges such as the high initial and maintenance costs, uncertainty due to environmental sensitivity, and low efficiency of these systems [1]. Despite an enormous amount of solar energy on the Earth, it is low-density, so it needs to be concentrated to increase heat flux. This issue is more challenging in high latitudes, thus the solar systems should be optimized by solar concentrators [2].

While Parabolic Trough Concentrators (PTC) are the most common and mature Concentereted Solar Power (CSP) technology [3],[4], the high cost of manufacturing and the sun-tracking system, heat loss problems, and the maximum yield of 60% make them unprofitable for urban areas.

On the other hand, lenses are reported to be comparable to an ideal concentrator with greater reliability [5], the most effective way to make full use of sunlight [6], less sensitive to the environment than exposed one [7],[8], higher thermal efficiency at a high-temperature for costs reduction [9], more cost-effective [10], and will bring a breakthrough of commercial solar energy in the near future [11], [12]. However, the complex knowledge of making large-scale glassy or Fresnel lenses has been an obstacle to use them in the building sector to supply domestic hot water and heating loads of buildings. To tackle the manufacturing challenge, Fresnel lenses have been introduced with cheaper costs but very limited acceptance angle, typically between 0.5 to10 degrees [13], and challenging to achieve a high concentration ratio and short focal length [14].

This research study aims to fill this gap by introducing and validating a new solar concentrator in the context of sustainable architecture in Tallinn, the capital city of Estonia (Lat. 59°26'N Lon. 24°45'E).

In this research, the proposed solar concentrator is a liquid lens that provides the benefits of lenses at an affordable price with underneath greenhouse effect and no need for expensive solar tracking systems.

2. Materials of the study, context, and solar concentrators

In this research, two office buildings in Tallinn, Estonia, with the same location, environment, and energy consumption but different rooftop CSP, one with a PTC and the other with a Water Lens, are compared. The comparison is based on the portion of the building's energy consumption generated by CSPs and the reduced CO_2 emissions over a year.

In Estonia, Domestic hot water production in summer is an acceptable choice among solar energy usage experts. In this country, solar energy is capable of covering approximately half of the domestic hot water needs of buildings [15].

2.1. Parabolic Trough Reflector

Although PTCs are more used by architects, the high costs of manufacturing, operation, expensive intercept mechanism and orientation system, and the heat loss by wind due to the exposed receiver, plus the maximum yield of 60%, causes to occupy more area, and as a result is unprofitable in urban contexts.

2.2. Liquid lenses

Liquid lenses [16], [17] are solar concentrators with cost-effective character, which contain plastic foil [18] or a glass layer with a Plano-convex lens shape [19] and the possibility of designing linear liquid lenses [20]. The fundamental advantages of this type of lense are described in [21].

The investigated system is addressed as a water lens instead of a liquid lens to be much cheaper for use in the building sector. The schematic drawing of the concentrator units is shown in Figure 1.

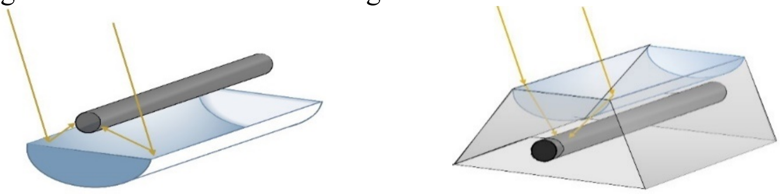

Figure 1 *Parabolic Trough Reflector (PTC) (left), and Water Lens (WL) (right)*

As shown in Fig. 1, the underneath closed space of the liquid lens can produce the greenhouse effect phenomenon, which helps to keep the receiver unexposed to the surrounded environment. This greenhouse effect not only can protect and prevent the receiver from wind heat loss but also can save the wasted energy due to abrasions of the lens by using Phase Change Materials (PCM).

Since the focal point of the lens is moving by the sun's movement during the day, this system does not require any sun-tracking system. Therefore, just changing the receiver's position in a designed path with a timer is enough. These advantages are the essential features of this solar concentrator.

3. Methodology

The research methodology is based on numerical data, the physics of light equations for an optical instrument, and software simulation by TracePro software from Lambda Research, USA, over a year.

The water lens is designed and optimized by the interactive optimizer in TracePro software to be more efficient and effective and has a width of 28 cm, a height of 1cm, and 1m in length.

3.1. Output calculation based on physics of light

When the incident light comes to the liquid lens, after decreasing the reflected portion, the remaining disperse, absorb, and pass through the liquid to be concentrated in the focal point.

The optical efficiency of a lens η_{op} is defined by the fraction of radiant power at its input aperture P_{in} which reaches its output P_{out} [22]: $\eta_{op} = P_{out}/P_{in}$ (1)

The amount of collected light at the focal point should be calculated by simulating the sun movement over a year to obtain the incident angle. The formula for calculating incident angle for a horizontal surface is: $\cos\beta z = \sin\delta \cdot \sin\theta + \cos\delta \cdot \cos\theta \cdot \cos\omega$ (2)

where β is the incident angle, ϒ is the solar azimuth, s is the slop angle, δ is the solar declination, ω is the hour angle, and θ is the latitude (Tallinn: θ = 59.436962). The solar declination angle δ can be calculated by the following formula [23]: $\delta = 23.45 \sin(360/365.(284+n))$ (3)

To calculate the hour-angle ω, the following equations can be used [24]: $\omega = \pm 0.25(\text{minutes})$ (4)
where minutes are the number of minutes from solar noon. The solar azimuth angle ϒ, which is the height of the sun, can be obtained by this formula: $\sin \Upsilon = \frac{\cos \delta . \sin \omega}{\cos \alpha}$ (5)
where α is the solar altitude as describe following: $\sin \alpha = \sin\delta . \sin\theta + \cos\delta . \cos\theta . \cos \omega$ (6)

For simplifying the calculation, every month's middle day in the solar calendar will be assumed. After calculation of the incident angle, the reflection percentage should be calculated. The reflection of light is known as Fresnel reflection, which describes what fraction of the light is reflected, which is given by the reflectance or reflectivity, R, and what fraction is refracted (i.e., transmitted) given by the transmittance or transmissivity, T, and reflectance for p-polarized light [25]:

$$R_s = \left[\frac{n_1 \cos \Theta_i - n_2 \cos \Theta_t}{n_1 \cos \Theta_i + n_2 \cos \Theta_t}\right]^2, \quad R_p = \left[\frac{Z_2 \cos \Theta_t - Z_1 \cos \Theta_t}{Z_2 \cos \Theta_t + Z_1 \cos \Theta_i}\right]^2 \quad (7)$$

If the incident light is unpolarised (containing an equal mix of s and p polarisations), the reflectance is: $R = \frac{1}{2}(R_s + R_p)$. (8)
where θi is incident angle βz is the incident angle on a horizontal surface, and θt describes as Snell's law. For clear water, which is filled in this research's water lens, n2 is around 1.333.

The amount of light attenuation is shown with the extinction coefficient. Extinction coefficient refers to several different measures of the absorption of the light in a medium: $I_z = I_0 \, e^{-kz}$ (9)
where I_z is irradiation intensity in the height of z and I_0 is irradiation intensity just below the water surface, K is attenuation coefficient, which is 0.02 for pure water. Moreover, to simplify the calculation, the centroid of the object, which is the intersection of the hyperplane that divides the height into two parts of equal moment, has been considered the representative height.

The maximum output temperature reported in Table 2 is the ambient temperature plus dT= Q/MC (10)where dT is the added temperature (°C), M is the receiver tube mass, and C is the heat capacity (J/K).

3.2. Output calculation based on software simulation for the full ray-tracing solar assessment
For the software simulation, the method is Monte Carlo Ray-tracing assessment for the optimized solar system in the interactive optimizer and simulating with the solar emulator in TracePro software.

The water lens has been modeled in this software, and all the default liquid properties and water material are attributed to the model. Then the solar emulator's setup for the latitude and longitude of Tallinn in each hour of every solar calendar's middle day simulated with 1000 W/m^2 solar irradiation, wavelength of 0.55 µm, and the number of rays of 1000. A receiver tube with 0.02m inner radius, 0.01m thickness, 1.2m length, and default perfect absorber properties have been placed in the focal point of each simulation. The irradiance map analysis is shown in Fig 2 for April 4th of at 12 o'clock.

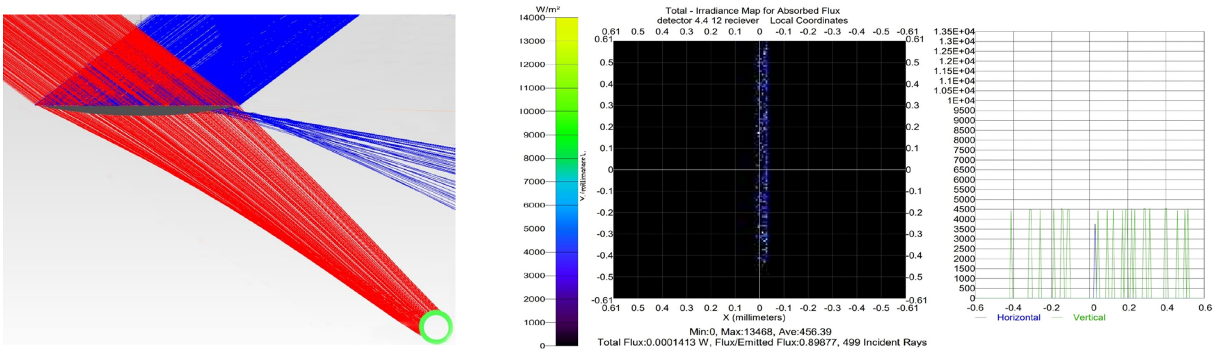

Figure 2 *TracePro simulation (left), and the irradiance map analysis (right) show 89% efficiency on April 4th at 12.*

3.3. The environmental sensitivity and wind-heat loss
Since the focal point of the PTC is exposed to the air, the wind causes heat loss. As it is shown in Table 2, the heat loss obtained by Newton's Law of Cooling equation for convection is: $q = hc.A.dT$ (11)

where q is the heat transferred (W), A is the heat transfer area (m2), h is the convective heat transfer coefficient (W/m2°C), and dT is the temperature difference between the surface and the bulk fluid (°C).

The amount of hc for air flow can be approximated to: $hc=12.12-1.16v+11.6v^{1/2}$ (12)

where v is the relative speed between the object surface and air (m/s).

4. Result and discussion

Table 1 shows the efficiency of the water lens with physics equations and simulation on April 4th. Figure 3 shows the comparison of efficiencies of physics equations and simulation for the water lens.

***Table 1** Hourly efficiency of April 4th for the proposed water lens as a solar concentrator*

Hour	Hour angle	Solar altitude	Solar azimuth	Incident angle	Hourly radiation	Ambient temperature	Wind speed	Reflect fraction	Entered radiation	Irradiation intensity	Receiver irradiation	Output efficiency		TracePro efficiency
H	ω	α	ϒ	ßz	W/m2*h	C°	m/s	%	W/m2*h	$I_Z = I_0 e^{-kz}$	$I_t - I_z$	%		%
6 am	-90	4.82	-84.40	85.18	32.00	1.02	4.90	0.70	9.65	31.90	9.62	0.30		0.00
7 am	-75	12.41	-74.01	77.59	64.00	1.37	5.21	0.33	43.00	63.81	42.87	0.67		0.00
8 am	-60	19.70	-59.53	70.30	119.00	1.71	5.52	0.14	102.17	118.64	101.87	0.86		0.24
9 am	-45	26.22	-44.73	63.78	157.00	2.05	5.83	0.10	142.01	156.53	141.58	0.90		0.51
10 am	-30	31.49	-29.84	58.51	152.00	2.08	5.71	0.04	145.34	151.54	144.90	0.95		0.71
11 am	-15	34.95	-14.93	55.05	153.00	2.11	5.59	0.03	149.13	152.54	148.68	0.97		0.85
12 pm	0	36.17	0.00	53.83	139.00	2.14	5.46	0.07	129.14	138.58	128.76	0.93		0.89
13 pm	-15	34.95	-14.93	55.05	134.00	2.14	4.55	0.03	149.13	152.54	148.68	0.97		0.91
14 pm	-30	31.49	-29.84	58.51	63.00	2.14	3.63	0.04	145.34	151.54	128.76	0.95		0.91
15 pm	-45	26.22	-44.73	63.78	31.00	2.13	2.72	0.10	142.01	156.53	148.68	0.90		0.90
16 pm	-60	19.70	-59.53	70.30	13.00	1.59	2.76	0.14	102.17	118.64	128.76	0.86		0.81
17 pm	-75	12.41	-74.01	77.59	0.00	1.06	2.80	0.33	43.00	63.81	148.68	0.67		0.67
18 pm	-90	4.82	-84.40	85.18	0.00	0.52	2.84	0.70	9.65	31.90	128.76	0.30		0.45

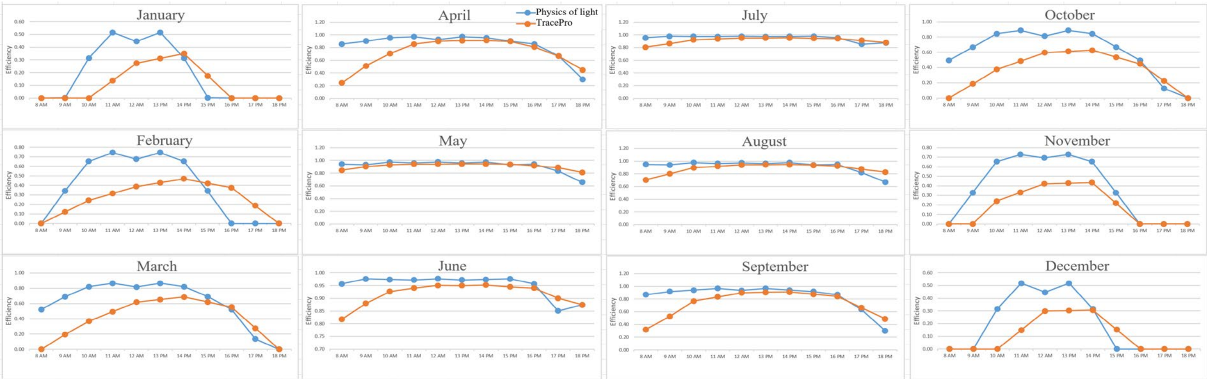

***Figure 3** The comparison of efficiencies of equations and simulation on the middle day of each solar calendar's month*

As it is presented in Fig 3, the correspondence of April to September, which are the most important months regarding to the amount of radiation, is acceptable. The results confidence is measured through validation indices and for the whole year obtained 0.167 and for the aforementioned months is 0.066.

Since the calculation and simulation for the whole day of the most important months showed a good similarity, the middle day of any month of solar calender is considered as a representive day for each month to estimate the annual integrated heat output. This simplification caused the simulation for any hour of each month to be less time consuming and the results were acceptable for transferring the specific heat power of each month to the annual integrated heat output. Moreover, as Figure 3 shows, since the outputs are estimated for every consecutive month, this generalization for simplifying the calculation and simulation is not imprecise and incorrect, especially for April to September, which are the most important months regarding the amount of radiation.

Table 2 shows the annual efficiency, output energy in kWh/m^2, and output temperature for both solar concentrators. Since the PTC has a solar tracking system, it `is supposed to be an ideal PTC that has the maximum energy yield of PTCs, 60%, with the wind heat loss for any hour of a year. As it can be seen, the maximum output temperature of the water lens is 54.54°C more than PTC just for a solar system with a 28 cm^2 area. Moreover, the annual output energy is 1.04 MWh/m^2more, and the efficiency is at least 6% more than PTC, considering PTC's heat loss by the wind.

Table 2 *Annual efficiency, output energy, and temperature of both concentrators*

Subject	Daily radiation	Daily mean temperature	Wind speed	Physics of light daily efficiency	TracePro daily efficiency	Water Lens output energy	Water Lens max temperature	PTC output energy	PTC max temperature
Unit	W/m2*h	C°	m/s	%	%	kWh/m2	C°	kWh/m2	C°
4-Apr	1057.00	1.70	4.42	0.84	0.71	6.8975	43.88	2.9407	10.72
5-May	1802.00	9.31	4.13	0.94	0.89	15.4769	75.08	8.2691	35.62
5-Jun	2260.00	11.78	4.71	0.96	0.92	18.5075	99.70	9.3984	41.06
6-Jul	2108.00	18.43	4.83	0.96	0.91	16.9568	106.92	11.4837	52.38
6-Aug	2109.00	18.50	2.89	0.89	0.88	15.8877	88.67	10.7492	50.30
6-Sep	1858.00	12.91	2.49	0.90	0.73	12.7462	73.06	8.3648	37.34
7-Oct	921.00	5.38	2.39	0.69	0.45	3.2416	40.69	3.6305	22.20
6-Nov	242.00	5.30	3.05	0.63	0.34	0.2477	24.33	0.8520	10.05
6-Dec	80.00	6.26	9.67	0.36	0.24	0.0942	25.74	0.6453	14.11
5-Jan	80.00	-9.90	2.72	0.36	0.25	0.0862	18.02	00.00	1.02
4-Feb	497.00	-0.08	4.99	0.46	0.33	1.2458	23.82	1.1491	5.94
6-Mar	518.82	0.29	3.66	0.69	0.50	1.7038	26.29	1.2470	6.37
				0.77 average	0.66 average	2831.5445 Annual output	106.92 max temp.	1786.3660 Annual output	52.38 max temp.

4.1. Reduced CO_2 emissions over a year

The comparison of this research is based on the portion of the building's energy consumption generated by CSPs, which is estimated as 1.04 kWh/m^2 over a year, and the annual reduced CO_2 emissions can be estimated by the amount of CO_2 that emissions through power generation by fossil fuels, which is 417 g/kW. Therefore the reduced CO_2 emissions are estimated to be 43.368 kg over a year.

4.2. Supplying Domestic Hot Water (DHW) in buildings

Generally, a hot water supplier system by renewable energy sources is one of the main solutions for achieving a fossil-free heating sector, specially when it comes to the summer time when a building has no need to heating system. In Estonia, applying solar collectors to produce domestic hot water leads to saving in total 5–15 % of the heat demand, and in the case of supplying space heating, it is estimated that 20 – 60 % of the total household heat consumption will be saved [15]. As it is described in Figure 3, the similarity of output energy of all the days of each month from April to September is acceptable and this caused to estimate the power generation for DHW by the average monthly output energy of the solar system. Then, as it is shown in Table 2, the solar system which is the subject of this study can be an affordable supplier of domestic hot water for buildings in Tallinn, in the period of April to September.

4.3. Generalization of the results for all latitudes

The modeling of the water lens for different latitudes are shown in Table 3:

Table 3 *Efficiency of the proposed water lens for different latitudes*

Latitude	efficiency	Latitude	efficiency	Latitude	efficiency	Latitude	Efficiency	Latitude	efficiency	Latitude	efficiency
θ	%	θ	%	θ	%	θ	%	θ	%	θ	%
1	74.81	11	76.9	21	76.75	31	75.12	41	72.86	51	66.72
2	75.14	12	76.75	22	77.02	32	74.72	42	72.71	52	65.98
3	7579	13	76.83	23	77.05	33	74.82	43	71.89	53	65.78
4	76	14	77.02	24	76.68	34	74.73	44	71.5	54	63.92
5	76.29	15	77.26	25	76.66	35	74.61	45	71.08	55	61.62
6	76.36	16	77.44	26	76.67	36	74.42	46	70.01	56	60.99
7	76.07	17	77.19	27	76.68	37	74.24	47	68.94	57	60.37
8	76.28	18	76.57	28	76.72	38	74.29	48	68.31	58	58.67
9	76.66	19	76.58	29	76.64	39	73.77	49	68.2	59	57.28
10	76.87	20	76.69	30	75.95	40	72.96	50	67.71	60	56.44

As table 3 indicates, the water lens is still productive in high latitudes where mirrors are not operative.

5. Conclusions and future developments

This research is one of the first studies about using water lenses in a sustainable building. The results show that although concave mirrors are more used in zero-energy buildings, water lenses are more efficient and effective: first, water lenses are about 8% more efficient and require less area. Second, the output temperature of water lenses is higher than that of mirrors, even though they do not require expensive electromechanical solar tracking systems, with lower initial and maintenance costs. Third, higher annual efficiency, due to the underneath greenhouse effect, make them less sensitive to the environment, such as wind, and provides the opportunity to save and recycle the wasted energy, especially in late evenings and winters. Lastly, modeling at other latitudes shows the water lenses are more productive even in high latitudes where mirrors are not operative. These advantages make them more reliable for enhancing the exploitation of solar energy potential in sustainable architecture, especially in high latitude countries.

Acknowledgment
"This work has been supported by the European Commission through the H2020 project Finest Twins (grant No. 856602)."

References

[1] Kabir, E.; Kumar, P.; Kumar, S.; Adelodun, A.A.; Kim, K. Solar energy: Potential and future prospects. Renew. Sustain. Energy Rev. 2018, 82, 894–900
[2] Wang, Gang, et al. "Experimental and optical performances of a solar CPV device using a linear Fresnel reflector concentrator." Renewable Energy 146 (2020): 2351-2361.
[3] Bellos, E., et al. "Thermal enhancement of solar parabolic trough collectors by using nanofluids and converging-diverging absorber tube." Renewable Energy 94 (2016): 213-222.
[4] Chacartegui, R., et al. "Analysis of two heat storage integrations for an Organic Rankine Cycle Parabolic trough solar power plant." Energy Conversion and Management 125 (2016): 353-36
[5] Kritchman, E. M., A. A. Friesem, and G. Yekutieli. "Efficient Fresnel lens for solar concentration." Solar Energy 22.2 (1979): 119-123.
[6] Xie, W. T., et al. "Concentrated solar energy applications using Fresnel lenses: A review." Renewable and Sustainable Energy Reviews 15.6 (2011): 2588-2606.
[7] Collares-Pereira, M. "High temperature solar collector with optimal concentration: non-focusing Fresnel lens with secondary concentrator." Solar Energy 23.5 (1979): 409-420.
[8] H.Zarrinkafsh, "Cable Structure Aided Water Lens For Solar Concentration", IR 95246, Validated by Iranian Research Organization for Science and Technology (IROST), IRIPO, 2017
[9] Zhai, H., et al. "Experimental investigation and analysis on a concentrating solar collector using linear Fresnel lens." Energy Conversion and Management 51.1 (2010): 48-55.
[10] Giostri, Andrea, et al. "Comparison of two linear collectors in solar thermal plants: parabolic trough versus Fresnel." Journal of Solar Energy Engineering 135.1 (2013): 011001.
[11] Madhugiri, Gaurav A., and S. R. Karale. "High solar energy concentration with a Fresnel lens." A Review. Int. J. Mod. Eng. Res 2 (2012): 1381-1385.
[12] Okulu, Keçiborlu Meslek Yüksek, and Süleyman Demirel Üniversitesi Teknoloji Fakültesi Enerji. "Experimental investigation of a linear Fresnel Collector." (2014).
[13] Zheng, Cheng, et al. "A new optical concentrator design and analysis for rooftop solar applications." Nonimaging Optics: Efficient Design for Illumination and Solar Concentration XII. Vol. 9572. International Society for Optics and Photonics, 2015.
[14] Zheng, Cheng, et al. "Design and indoor testing of a compact optical concentrator." Optical Engineering 56.1 (2017): 015102.
[15] Sustainable Energy Vision for Estonia, A path to make Estonian energy independent and sustainable by 2050, INFORSE-Europe, March, 2011.
[16] Wei, Kang, et al. "Focus-tunable liquid lens with an aspherical membrane for improved central and peripheral resolutions at high diopters." Optics express 24.4 (2016): 3929-3939.
[17] Downing, John. "Effects of Light Absorption and Scattering in Water Samples on OBS Measurements." Campbell Scientifici, Inc (2008).
[18] Ren, Hongwen, and Shin-Tson Wu. "Variable-focus liquid lens." Optics Express 15.10 (2007): 5931-5936.
[19] Mondol, A. S., B. Vogel, and G. Bastian. "Large scale water lens for solar concentration." Optics express 23.11 (2015): A692-A708.
[20] Rinaldi, F., et al. "Comparison of linear and point focus collectors in solar power plants." Energy Procedia 49 (2014): 1491-1500.
[21] Mondol, A. S., B. Vogel, and G. Bastian. "Large scale water lens for solar concentration." Optics express 23.11 (2015): A692-A708.
[22] Antón, I., Pachón, D., Sala, G., Characterization of optical collectors for concentration photovoltaic applications. Prog. Photovolt. Res. Appl. 2003.11, 387– 405. http://dx.doi.org/10.1002/pip.502.
[23] Duffie, John A., and William A. Beckman. "Solar engineering of thermal processes." (1980).
[24] Brock, Thomas D. "Calculating solar radiation for ecological studies." Ecological Modelling (1981): 1-19.
[25] Hecht, Eugene (1987). Optics (2nd ed.). Addison Wesley. ISBN 0-201-11609-X.